

# Thermoelectric Nanogenerators Based on Single Sb-Doped ZnO Micro/Nanobelts

Ya Yang,<sup>†</sup> Ken C. Pradel,<sup>†</sup> Qingshen Jing,<sup>†</sup> Jyh Ming Wu,<sup>†</sup> Fang Zhang,<sup>†</sup> Yusheng Zhou,<sup>†</sup> Yue Zhang,<sup>‡</sup> and Zhong Lin Wang<sup>†,§,\*</sup>

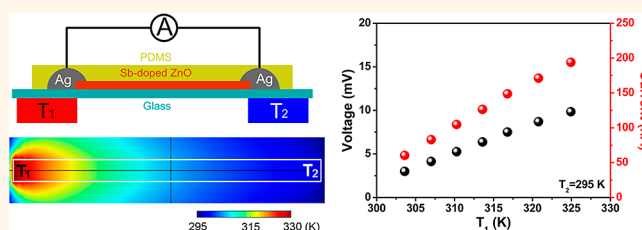
<sup>†</sup>School of Materials Science and Engineering, Georgia Institute of Technology, Atlanta, Georgia 30332-0245, United States, <sup>‡</sup>State Key Laboratory for Advanced Metals and Materials, School of Materials Science and Engineering, University of Science and Technology Beijing, 100083 Beijing, China, and <sup>§</sup>Beijing Institute of Nanoenergy and Nanosystems, Chinese Academy of Sciences, China

Harvesting waste energy in the living environment to power small electronic devices and systems is attracting increasing attention.<sup>1–3</sup> As the size of the devices has shrunk to the nanoscale, the power consumption can also decrease to a low level of nanowatts. The self-powered nanotechnology is to drive a nanodevice by scavenging energy from its working environment instead of a conventional battery.<sup>4</sup> Usually, we can obtain the light, mechanical, and heat energies from living environment. The piezoelectric nanogenerator (NG) has been extensively designed to transfer the mechanical energy into electric energy.<sup>5–7</sup> The nanowire solar cells can be used to transfer the light energy to electric energy.<sup>8,9</sup> Heat energy will be particularly important when other sources of energy, such as sun light or mechanical vibration, are not available.

Heat energy is a very conventional energy source in our living environment, with source in the engine of moving automobiles, the CPU of computers, human body, etc., all of which are normally wasted. The mechanism of a thermoelectric NG is to drive the charge carriers to flow in the circuit by keeping a thermal gradient in the device.<sup>10–12</sup> Usually, it is difficult for the nanowire thermoelectric devices to keep the temperature difference across a short distance.<sup>13</sup> An only possibility is to increase the length of a single nanowire to obtain a stable thermal gradient in the nanowire.

Nontoxic and low-cost oxides such as ZnO nanomaterials are promising for fabricating thermoelectric NGs because their excellent charge carrier transport properties are tunable *via* doping.<sup>14–16</sup> It has been reported that the Sb doping in ZnO micro/nanobelts can be used to enhance the

## ABSTRACT



We demonstrate a thermoelectric nanogenerator (NG) made from a single Sb-doped ZnO micro/nanobelt that generates an output power of about 1.94 nW under a temperature difference of 30 K between the two electrodes. A single Sb-doped ZnO microbelt was bonded at its ends on a glass substrate as a NG, which can give an output voltage of 10 mV and an output current of 194 nA. The single Sb-doped ZnO microbelt shows a Seebeck coefficient of about  $-350 \mu\text{V/K}$  and a high power factor of about  $3.2 \times 10^{-4} \text{ W/mK}^2$ . The fabricated NG demonstrated its potential to work as a self-powered temperature sensor with a reset time of about 9 s.

**KEYWORDS:** ZnO · micro/nanobelts · thermoelectric · nanogenerator · Sb-doped ZnO · temperature sensor

mechanical, electrical, and electromechanical properties.<sup>17–19</sup> Although the thermoelectric property of Al-doped ZnO nanoparticles has been investigated,<sup>20</sup> there are few studies about using a single Sb-doped ZnO micro/nanobelt for harvesting thermal energy. Here, a single Sb-doped ZnO microbelt with the length of larger than 3 mm was manipulated for fabricating a NG to investigate the output power and thermoelectric performance of Sb-doped ZnO. The output power of NG is about 1.94 nW under a temperature difference of 30 K. The Seebeck coefficient and power factor of a single Sb-doped ZnO microbelt are about  $-350 \mu\text{V/K}$  and  $3.2 \times 10^{-4} \text{ W/mK}^2$ , respectively. We also demonstrated that the fabricated NG can work as a self-powered temperature sensor.

\* Address correspondence to zlwang@gatech.edu.

Received for review May 7, 2012 and accepted June 28, 2012.

Published online June 29, 2012  
10.1021/nn302481p

© 2012 American Chemical Society

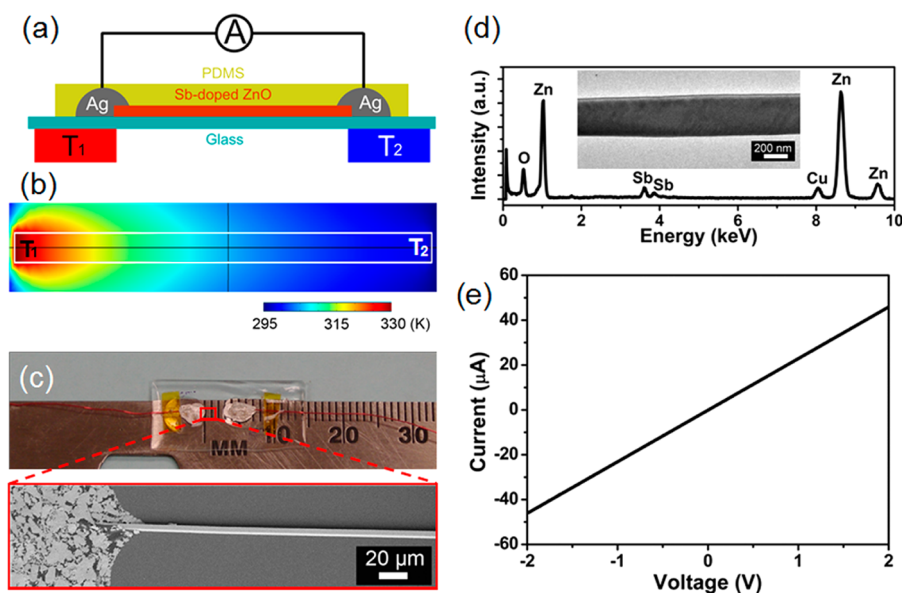


**Figure 1.** (a) Schematic diagram of a single Sb-doped ZnO microbelt NG. (b) Calculated temperature distribution along a glass substrate. (c) Photograph of the fabricated device and its corresponding enlarged SEM image. (d) EDS spectra of a single Sb-doped ZnO nanobelt. The inset shows a TEM image of the nanobelt. (e)  $I$ – $V$  characteristic of a fabricated NG.

## RESULTS AND DISCUSSION

The Sb-doped ZnO micro/nanobelts were synthesized by using a simple chemical vapor deposition method. The detailed growth method is given in the Experimental Section. The schematic of the thermoelectric NG is shown in Figure 1a. We chose large size microbelts for easy manipulation under an optical microscope. The same principle and methodology can apply to nanobelts. A long Sb-doped ZnO microbelt with a length of larger 3 mm was chosen under an optical microscope. A thin glass substrate was washed with deionized water and ethanol under sonication. The ZnO microbelt was placed on the glass substrate, and the two ends of the microbelt were then fixed tightly by the silver paste, where the distance between the two electrodes is 3 mm. A thin poly(dimethylsiloxane) (PDMS) layer was used to package the device to avoid the effect of atmosphere. Moreover, it can prevent the Sb-doped ZnO micro/nanobelt from contamination or corrosion. We can also easily move the device as a self-powered temperature sensor. Two heaters were fixed on the two electrodes, where only one heater was turned on to maintain a temperature gradient along the ZnO microbelt. Figure 1b shows a temperature distribution along a glass substrate (marked with white line) with a length of 3 mm by using COMSOL software. When one end of the glass was heated to 330 K, the other end of the glass is about 295 K. The experimental results also show that the temperature of one end of the glass substrate can be kept at 295 K when the other end of the glass substrate was heated to be below 340 K (Figure S1 in the Supporting Information).

Figure 1c shows an optical image of the fabricated NG. The distance between the two electrodes is about

3 mm. The enlarged SEM image shows that the width of the microbelt is about 10 μm, which was confirmed further from the corresponding AFM image (Figure S2). The EDS spectra in Figure 1d show that the Sb content in ZnO nanobelts was identified to be about 5%, which is consistent with our previous report.<sup>17</sup> The atomic ratio between Zn and O is about 2:1. The EDS line scale profile of Sb across a single Sb-doped ZnO nanobelt shows that the Sb doping is uniform (Figure S3). Figure 1e shows the  $I$ – $V$  characteristic of the NG. The contact between Ag and Sb-doped ZnO is Ohmic, which is important to obtain the low contact resistance. The fabricated NG has a good stability of  $I$ – $V$  characteristics, as shown in Figure S4.

When the temperature  $T_1$  at the left-hand side electrode of the NG was increased from 295 to 304 K, the temperature  $T_2$  at the right-hand side electrode was kept constant (295 K). As shown in Figure 2a, the difference of temperature at the two electrodes can produce an output voltage and current of about 3 mV and 60 nA, respectively. Moreover, when the temperature  $T_1$  at the left-hand side electrode of the NG was constant (295 K) and the temperature  $T_2$  at the right-hand side electrode was increased to 304 K, the output voltage and current signals were opposite, as shown in Figure 2b. We also performed the reversed voltage/current direction experiments, as presented in Figure S5. The output voltage and current values under the forward and reverse directions are nearly same. The results indicate that the observed voltage and current signals are from the fabricated NG. To confirm that the obtained signals are due to the Sb-doped ZnO microbelt, we tested the output voltage when there was no Sb-doped ZnO microbelt, as shown in Figure S6.

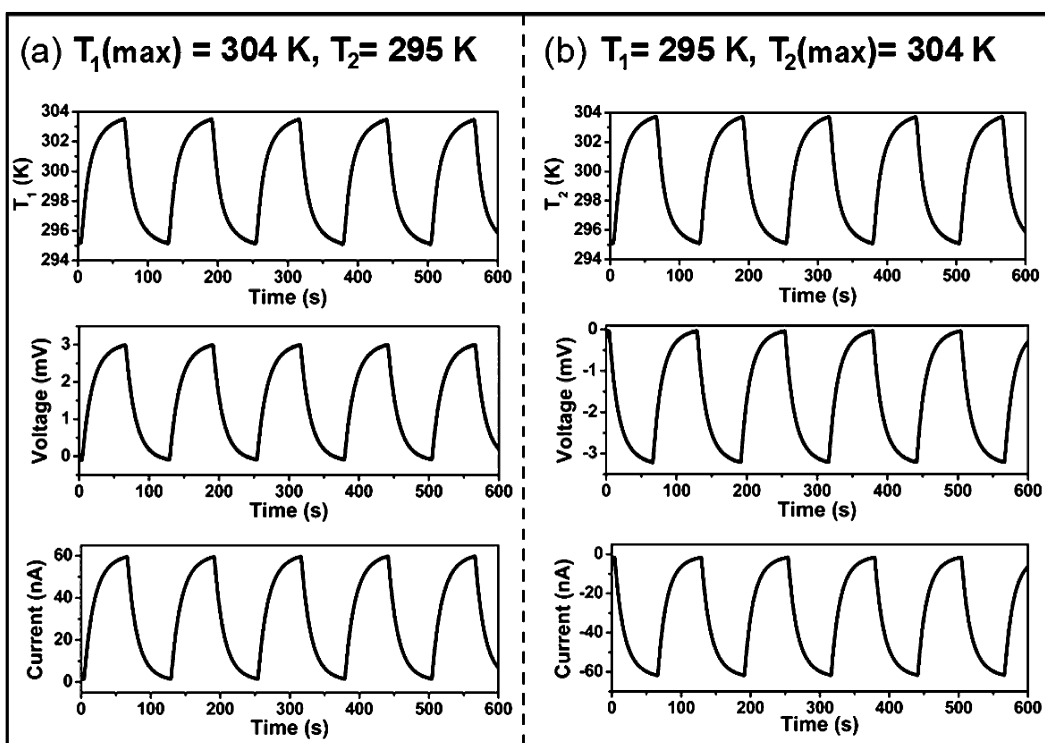


Figure 2. (a) Output voltage and current of the fabricated NG when the temperature  $T_2$  at the right-hand electrode is 295 K and the temperature  $T_1$  at the left-hand electrode periodically changed from 295 to 304 K. (b) Output voltage and current of the NG when the temperature  $T_1$  at the left-hand electrode is 295 K and the temperature  $T_2$  at the right-hand electrode periodically changed from 295 to 304 K.

The output voltage signals were not observed when the temperature at the left-hand side electrode was increased to 315 K and the temperature at the right-hand side electrode was 295 K. Our results indicate that the output signals were from the Sb-doped ZnO microbelt.

To investigate the output difference of the fabricated different devices, we measured another eight devices, as shown in Figure 3a. The output voltages of the devices are from 4 to 6 mV under a temperature difference of 14 K between two electrodes. To obtain the value of the contact resistance between the Ag electrode and the Sb-doped ZnO microbelt, a four-terminal measurement method was used.<sup>21</sup> Figure 3b shows both the two-terminal and four-terminal  $I$ - $V$  characteristics of a single microbelt in the inset, where the effect of contact resistance is visible. The two-terminal  $I$ - $V$  characteristic for this microbelt was measured by using the inner two electrodes, whereas the four-terminal  $I$ - $V$  plot was obtained by varying the current through the outer two electrodes and measuring the corresponding voltage drops between the inner two electrodes. The obtained contact resistance between the Ag and Sb-doped ZnO microbelt is about 4 k $\Omega$ , which is much smaller than the intrinsic resistance (35.5 k $\Omega$ ) of the single Sb-doped ZnO microbelt in Figure 1c,e. Since the resistance (100 M $\Omega$ ) of the used voltmeter is much larger than the contact resistance (4 k $\Omega$ ), the contact resistance has no contribution

to the measured voltage and Seebeck coefficient. Here,  $V_1/V_2 = (2R_C + R_V)/R_V$ , where  $V_1$  is the thermoelectric voltage,  $V_2$  is the measured voltage by using the voltmeter,  $R_C$  is the contact resistance, and  $R_V$  is the resistance of the voltmeter.

When the temperature at the right-hand electrode was 295 K, the increase of the temperature at the left-hand electrode can increase the output voltage/current of the NG. Figure S7 shows that, under the temperature of 325 K at the left electrode, the output voltage and current of the NG are up to about 10 mV and 194 nA, respectively. Figure 3c shows that the output voltage/current linearly increases with increasing temperature  $T_1$  at the left-hand electrode. The Seebeck coefficient can be obtained by a simple relationship of  $S = -\Delta V/\Delta T$ , where  $\Delta V$  is the thermoelectric voltage and  $\Delta T$  is the temperature difference.<sup>22</sup> The absolute Seebeck coefficient can be calibrated by using the positive Seebeck coefficient (+1.84  $\mu\text{V}/\text{K}$ ) of the Cu wire between the electrode and voltmeter. Figure 3d shows that the Seebeck coefficient of the single Sb-doped ZnO microbelt is about  $-350 \mu\text{V}/\text{K}$ , which is larger than that of Al-doped ZnO nanostructures ( $-300 \mu\text{V}/\text{K}$ ) at room temperature.<sup>20</sup> Figure S8 shows that the single Sb-doped ZnO microbelt exhibits a room temperature electrical conductivity of about  $2.7 \times 10^3 \Omega^{-1} \text{m}^{-1}$ , which is much larger than that of the nanostructured pure ZnO.<sup>23,24</sup> The Sb doping in ZnO can increase the electron concentration, resulting

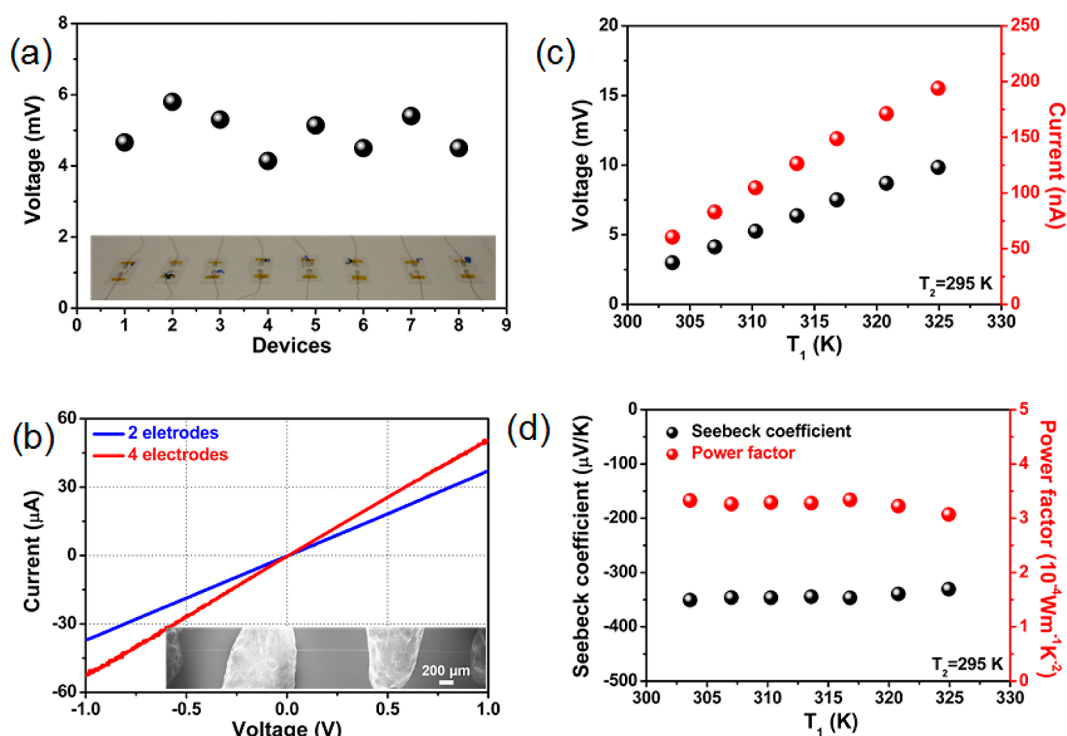


Figure 3. (a) Output voltages of the fabricated eight devices under a temperature difference of 14 K. The inset shows an optical image of the eight devices. (b) Two-terminal and four-terminal  $I$ - $V$  characteristics of a single Sb-doped microbelt. The inset shows a SEM image of the measurement structure. (c) Output voltage and current of a fabricated device under the different temperatures. (d) Seebeck coefficients and power factors under different temperatures. Here,  $T_1$  and  $T_2$  are the temperatures at the left- and right-hand side electrodes of the NG, respectively.

in an increase in the conductivity.<sup>25</sup> The power factors  $\alpha^2\sigma$  under the different temperatures are shown in Figure 3b, where  $\alpha$  is the Seebeck coefficient and  $\sigma$  is the electrical conductivity. The room temperature power factor of a single Sb-doped ZnO microbelt is about  $3.2 \times 10^{-4} \text{ W m}^{-1} \text{ K}^{-2}$ , which is 10 times larger than that of Al-doped ZnO nanostructures ( $0.18 \times 10^{-4} \text{ W m}^{-1} \text{ K}^{-2}$ ).<sup>20</sup>

The conversion efficiency  $\eta$  of a thermoelectric NG is typically defined as

$$\eta = \frac{\Delta T}{T_h} \times \frac{\sqrt{1+ZT} - 1}{\sqrt{1+ZT} + T_c/T_h} \quad (1)$$

where  $\Delta T = T_h - T_c$  is the temperature difference across the device,  $ZT = (\alpha^2 T)/(\rho\kappa)$  is the average material figure of merit,  $\alpha$  is the Seebeck coefficient,  $\rho$  is the resistivity, and  $\kappa$  is the thermal conductivity.<sup>26</sup> Under a temperature difference of 30 K, the conversion efficiency  $\eta$  of the fabricated NG is about 0.32%, where the thermal conductivity of 0.745 W/mK for ZnO micro-materials was used.<sup>27</sup> The actual conversion efficiency of the NG will be slightly smaller than the calculated value.

An important application of the NG is that it can work as a self-powered temperature sensor. Figure 4a shows an optical image, where a finger was used to touch one electrode of the NG. There was an output current of about 1.25 nA due to the temperature

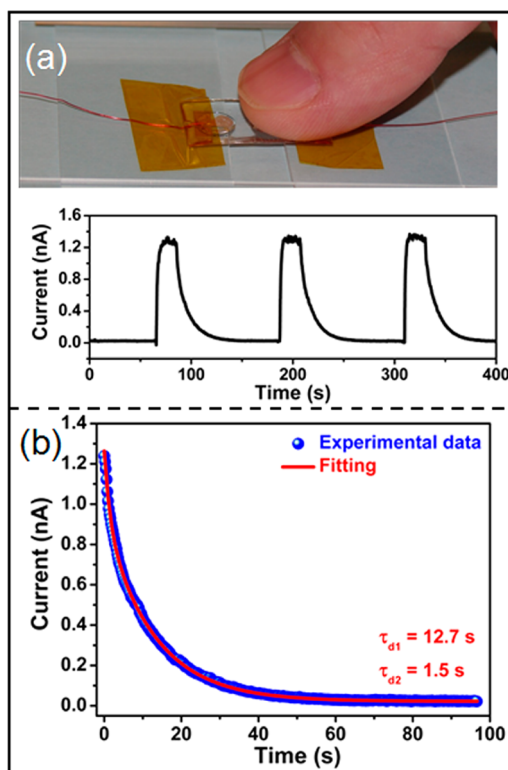


Figure 4. (a) Optical image when a finger touched one electrode of the NG and its corresponding output current. (b)  $I$ - $T$  curve when the finger was moved out.

difference between the two electrodes. When the finger was moved out, the output current will be recovered to 0. By fitting the  $I-T$  curves in Figure 4b, the decay time of temperature response follows a second-order exponential decay function,<sup>28</sup> with the estimated time constant of  $\tau_{d1} = 12.7$  s and  $\tau_{d2} = 1.5$  s, and relative weight factors of 75% and 25%, respectively. The decay mechanism in Figure 4b is related to the temperature dissipation in the single Sb-doped ZnO microbelt. The reset time is defined as the time need to recover to  $1/e$  (37%). The value of the temperature sensor is about 9 s.

## CONCLUSION

In summary, we have demonstrated a single Sb-doped ZnO micro/nanobelt NG for thermoelectric energy conversion. Under a temperature difference of 30 K between two electrodes, the NG can produce an output voltage of about 10 mV and an output current of 194 nA. The single Sb-doped ZnO microbelt shows a Seebeck coefficient of about  $-350 \mu\text{V/K}$  and a power factor of about  $3.2 \times 10^{-4} \text{ W/mK}^2$ , respectively. The results support the applications of single Sb-doped ZnO micro/nanobelts in thermoelectric energy conversion and self-powered nanodevices/systems.

## EXPERIMENTAL SECTION

**Synthesis of Sb-Doped ZnO Micro/Nanobelts.** First, Zn powder (purity 99.9%),  $\text{Sb}_2\text{O}_3$  powder (purity of 99.999%), and graphite powder with a molar ratio of 4:1:2 were fully ground into a mixture before being loaded in a quartz boat. A cleaned Si wafer was used as the substrate and fixed on the boat with the polished side facing the powders. The temperature and the growth time were maintained at 930 °C and 20 min, respectively. The flow rates of Ar and  $\text{O}_2$  are 290 and 10 sccm, respectively (sccm denotes standard cubic centimeter per minute at STP). After the reaction, a white-colored film-like product was obtained on the Si substrate. The Sb-doped ZnO micro/nanobelts were characterized by scanning electron microscopy (SEM, LEO1530, Japan), transmission electron microscopy (TEM, Hitachi HF2000, Japan), and energy-dispersive X-ray spectroscopy (EDS).

**Fabrication and Measurements of the Devices.** A single long (>3 mm) Sb-doped ZnO microbelt was placed on a thin glass substrate. The two ends of the microbelt were fixed by silver pastes, which were used as electrodes. A thin layer of PDMS was used to package the device. The output signals of the thermoelectric NG were measured by using a low-noise voltage pre-amplifier (Stanford Research System model SR560) and a low-noise current preamplifier (Stanford Research System model SR570).

**Conflict of Interest:** The authors declare no competing financial interest.

**Acknowledgment.** This work was supported by Air Force, U.S. Department of Energy, Office of Basic Energy Sciences, Division of Materials Sciences and Engineering under Award DE-FG02-07ER46394, and NSF (CMMI 0403671).

**Supporting Information Available:** (1) The temperature difference between two electrodes of the fabricated device. (2) The AFM image of the single Sb-doped ZnO microbelt and its corresponding cross-section profile. (3) A TEM image of a single Sb-doped ZnO nanobelt and the EDX line scale profile of Sb across the single nanobelt. (4) The stability of the  $I-V$  characteristics of the NG. (5) The output current and voltage of the NG under the reversed electrode condition. (6) The controlled experiment: the output voltage of the device without the Sb-doped ZnO microbelt. (7) The output voltage and current of the fabricated NG under a temperature difference of 30 K. (8) The  $I-V$  characteristics of the Sb-doped ZnO microbelt under the different temperatures and the corresponding electrical conductivities. This material is available free of charge via the Internet at <http://pubs.acs.org>.

## REFERENCES AND NOTES

1. Katz, E.; Bückmann, A. F.; Willner, I. Self-Powered Enzyme-Based Biosensors. *J. Am. Chem. Soc.* **2001**, *123*, 10752–10753.

2. Dondi, D.; Bertacchini, A.; Larcher, L.; Brunelli, D.; Benini, L. Modeling and Optimization of a Solar Energy Harvester System for Self Powered Wireless Sensor Networks. *IEEE Trans. Ind. Electron.* **2008**, *55*, 2759–2766.
3. Hu, Y.; Zhang, Y.; Xu, C.; Lin, L.; Snyder, R. L.; Wang, Z. L. Self-Powered System with Wireless Data Transmission. *Nano Lett.* **2011**, *11*, 2572–2577.
4. Xu, S.; Qin, Y.; Xu, C.; Wei, Y.; Yang, R.; Wang, Z. L. Self-Powered Nanowire Devices. *Nat. Nanotechnol.* **2010**, *5*, 366–373.
5. Wang, Z. L.; Song, J. H. Piezoelectric Nanogenerators Based on Zinc Oxide Nanowire Arrays. *Science* **2006**, *312*, 242–246.
6. Qin, Y.; Wang, X. D.; Wang, Z. L. Microfibre–Nanowire Hybrid Structure for Energy Scavenging. *Nature* **2008**, *451*, 809–813.
7. Hu, Y.; Lin, L.; Zhang, Y.; Wang, Z. L. Replacing a Battery by a Nanogenerator with 20 V Output. *Adv. Mater.* **2012**, *24*, 110–114.
8. Tian, B.; Zheng, X.; Kempa, T. J.; Fang, Y.; Yu, N.; Yu, G.; Huang, J.; Lieber, C. M. Coaxial Silicon Nanowires as Solar Cells and Nanoelectronic Power Sources. *Nature* **2007**, *449*, 885–890.
9. Yang, Y.; Guo, W.; Zhang, Y.; Ding, Y.; Wang, X.; Wang, Z. L. Piezotronic Effect on the Output Voltage of P3HT/ZnO Micro/Nanowire Heterojunction Solar Cells. *Nano Lett.* **2011**, *11*, 4812–4817.
10. Yan, X.; Poudel, B.; Ma, Y.; Liu, W. S.; Joshi, G.; Wang, H.; Lan, Y. C.; Wang, D. Z.; Chen, G.; Ren, Z. F. Experimental Studies on Anisotropic Thermoelectric Properties and Structures of n-Type  $\text{Bi}_2\text{Te}_{2.7}\text{Se}_{0.3}$ . *Nano Lett.* **2010**, *10*, 3373–3378.
11. Zhang, Y.; Dresselhaus, M. S.; Shi, Y.; Ren, Z.; Chen, G. High Thermoelectric Figure-of-Merit in Kondo Insulator Nanowires at Low Temperatures. *Nano Lett.* **2011**, *11*, 1166–1170.
12. Zebarjadi, M.; Esfarjani, K.; Dresselhaus, M. S.; Ren, Z. F.; Chen, G. Perspectives on Thermoelectrics: From Fundamentals to Device Applications. *Energy Environ. Sci.* **2012**, *5*, 5147–5162.
13. Sebald, G.; Guyomar, D.; Agbossou, A. On Thermoelectric and Pyroelectric Energy Harvesting. *Smart Mater. Struct.* **2009**, *18*, 125006.
14. Thompson, R. S.; Li, D.; Witte, C. M.; Lu, J. G. Weak Localization and Electron–Electron Interactions in Indium-Doped ZnO Nanowires. *Nano Lett.* **2009**, *9*, 3991–3995.
15. Yang, Y.; Qi, J.; Liao, Q.; Zhang, Y.; Tang, L.; Qin, Z. Synthesis and Characterization of Sb-Doped ZnO Nanobelts with Single-Side Zigzag Boundaries. *J. Phys. Chem. C* **2008**, *112*, 17916–17919.
16. Zhou, M.; Zhu, H.; Jiao, Y.; Rao, Y.; Hark, S.; Liu, Y.; Peng, L.; Li, Q. Optical and Electrical Properties of Ga-Doped ZnO Nanowire Arrays on Conducting Substrates. *J. Phys. Chem. C* **2009**, *113*, 8945–8947.
17. Yang, Y.; Qi, J.; Guo, W.; Liao, Q.; Zhang, Y. Mechanical and Longitudinal Electromechanical Properties of Sb-Doped ZnO Nanobelts. *CrystEngComm* **2010**, *12*, 2005–2007.

18. Yang, Y.; Guo, W.; Qi, J.; Zhao, J.; Zhang, Y. Self-Powered Ultraviolet Photodetector Based on a Single Sb-Doped ZnO Nanobelt. *Appl. Phys. Lett.* **2010**, *97*, 223113.
19. Yang, Y.; Qi, J.; Zhang, Y.; Liao, Q.; Tang, L.; Qin, Z. Controllable Fabrication and Electromechanical Characterization of Single Crystalline Sb-Doped ZnO Nanobelts. *Appl. Phys. Lett.* **2008**, *92*, 183117.
20. Jood, P.; Mehta, R. J.; Zhang, Y.; Peleckis, G.; Wang, X.; Siegel, R. W.; Tasciuc, T. B.; Dou, S. X.; Ramanath, G. Al-Doped Zinc Oxide Nanocomposites with Enhanced Thermoelectric Properties. *Nano Lett.* **2011**, *11*, 4337–4342.
21. Liao, L.; Lin, Y. C.; Bao, M. Q.; Cheng, R.; Bai, J. W.; Liu, Y.; Qu, Y. Q.; Wang, K. L.; Huang, Y.; Duan, X. High Speed Graphene Transistors with a Self-Aligned Nanowire Gate. *Nature* **2010**, *467*, 305.
22. Lee, C.-H.; Yi, G.-C.; Zuev, Y. M.; Kim, P. Thermoelectric Power Measurements of Wide Band Gap Semiconducting Nanowires. *Appl. Phys. Lett.* **2009**, *94*, 022106.
23. Heo, Y. W.; Tien, L. C.; Norton, D. P. Electrical Transport Properties of Single ZnO Nanorods. *Appl. Phys. Lett.* **2004**, *85*, 2002–2004.
24. Goldberger, J.; Sirbully, D. J.; Law, M.; Yang, P. ZnO Nanowire Transistors. *J. Phys. Chem. B* **2005**, *109*, 9–14.
25. Park, K.; Seong, J. K.; Nahm, S. Improvement of Thermoelectric Properties with the Addition of Sb to ZnO. *J. Alloys Compd.* **2008**, *455*, 331–335.
26. Snyder, G. J. Thermoelectric Power Generation: Efficiency and Compatibility. In *Thermoelectric Handbook Macro to Nano*; Rowe, D. M., Ed.; CRC Press: Boca Raton, FL, 2006; Chapter 9.
27. Olorunyolemi, T.; Birnboim, A.; Carmel, Y.; Wilson, O. C., Jr.; Lloyd, I. K. Thermal Conductivity of Zinc Oxide: From Green to Sintered State. *J. Am. Ceram. Soc.* **2002**, *85*, 1249–1253.
28. Zhou, J.; Gu, Y.; Hu, Y.; Mai, W.; Yeh, P.-H.; Bao, G.; Sood, A. K.; Polla, D. L.; Wang, Z. L. Gigantic Enhancement in Response and Reset Time of ZnO UV Nanosensor by Utilizing Schottky Contact and Surface Functionalization. *Appl. Phys. Lett.* **2009**, *94*, 191103.